Alkyl 2-Benzothiazolyl Sulfide Ligated Dirhenium Complexes: Syntheses, Structure and Computational Study of [Re2(CO)8{μ,η1,η1-(R)SCNSC6H4}] (R = CH3 and C2H5)

Md. Wahidul Islam
Jahangirnagar University
Joyanta K. Saha
Jagannath University
Nikhil C. Bhoumik
Jahangirnagar University
Shafikul Islam (chem.shafik@juniv.edu)
Jahangirnagar University
Md. Manzurul Karim
Jahangirnagar University

Research Article

Keywords: Displacement reaction, Crystal structure, DFT calculation, Hirsfeld surface analysis

Posted Date: May 13th, 2021

DOI: https://doi.org/10.21203/rs.3.rs-498572/v1

Alkyl 2-benzothiazolyl sulfide ligated dirhenium complexes: syntheses, structure and computational study of $[Re_2(CO)_8\{\mu,\eta^1,\eta^1\text{-}(R)SCNSC_6H_4\}]$ (R = CH_3 and C_2H_5)

Md. Wahidul Islam[a] . Joyanta K. Saha[b] . Nikhil C. Bhoumik[c] . Shafikul Islam*[,a] . Md. Manzurul Karim[a]

a. Department of Chemistry, Jahangirnagar University, Savar, Dhaka-1342, Bangladesh.
b. Department of Chemistry, Jagannath University, Dhaka-1100, Bangladesh.
c. Wazed Miah Science Research Center, Jahangirnagar University, Savar, Dhaka-1342, Bangladesh.
* Corresponding author; Email: chem.shafik@juniv.edu

† Electronic Supplementary Information (ESI) available: CCDC 1976501 for compound **1** and CCDC 1976360 for compound **2**; Crystallographic data of compounds **1** and **2**, see DOI: ……..

GRAPHICAL ABSTRACT

Two novel alkyl 2-benzothiazolyl sulfide ligated dirhenium complexes having the general formula, $[Re_2(CO)_8\{\mu,\eta^1,\eta^1\text{-}(R)SCNSC_6H_4\}]$, were synthesized and structurally characterized, and some of their properties such as band gap, intermolecular interactions and close contact were studied with the help of computational method.

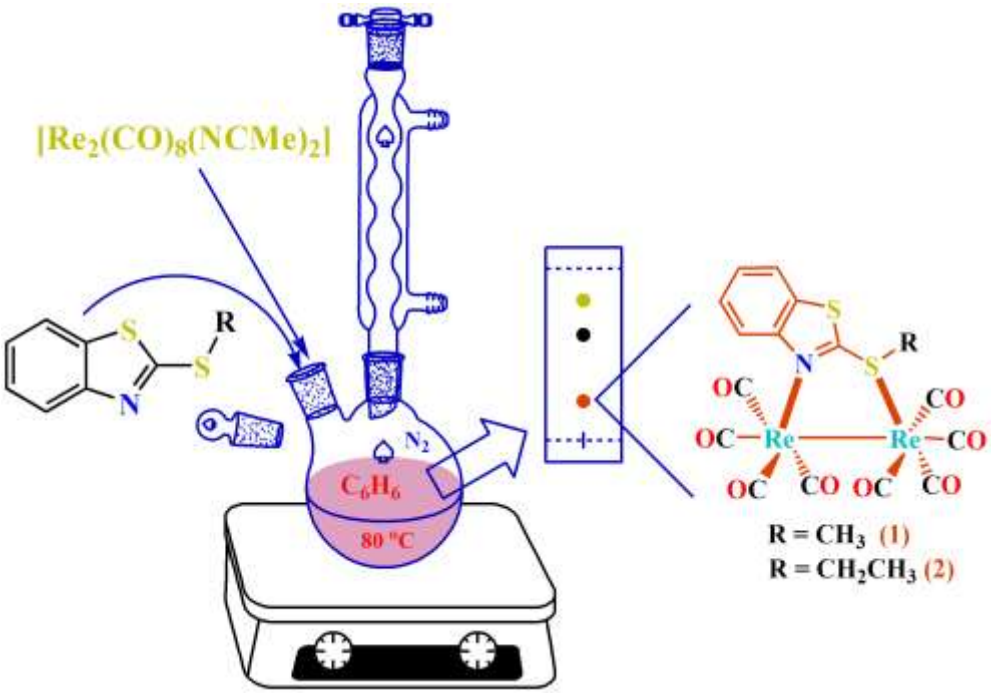

ABSTRACT

The synthesis of dirhenium complexes of 2-(methylthio)benzothiazole and 2-(ethylthio)benzothiazole and their X-ray crystal structures are reported. The complexes, $[Re_2(CO)_8\{\mu,\eta^1,\eta^1\text{-}(CH_3)SCNSC_6H_4\}]$ (**1**) and $[Re_2(CO)_8\{\mu,\eta^1,\eta^1\text{-}(C_2H_5)SCNSC_6H_4\}]$ (**2**) are isolated as orange crystals from the easy displacement of acetonitrile from the labile complex, $[Re_2(CO)_8(MeCN)_2]$ in moderate yields. The complexes were characterized by elemental analyses and spectroscopic method, and their structures were determined by single crystal X-ray diffraction method. The optimized bond lengths and bond angles of the complexes using DFT method are in good agreement with experimental X-ray crystallographic data. The HOMO and LUMO energy levels of complexes **1** and **2** were studied with the help of DFT method, and their energy gaps were found 3.08 and 3.13 eV, respectively. The Hirshfeld surface analysis was performed to study the intermolecular interaction, crystal packing, and identification of close contacts in both complexes.

Keywords: Displacement reaction, Crystal structure, DFT calculation, Hirsfeld surface analysis.

Introduction

The reactions of $Re_2(CO)_{10}$ with sulfur-containing ligands have been studied for several decades. For example, the reactions of $Re_2(CO)_{10}$ with pyridine-2-thiol [1], thioacetamide [2], thiobenzamide [2], diaryl disulfides [3], pyrimidine-2-thiol [4], 2-mercaptothiazoline [5], 2-mercaptobenzimidazole [5], 2-mercapto-1-methylimidazole [5], and 2-mercaptobenzoxazole [6] have been reported. Recent advances in research reveal the isolation of mixed metal [7-9] and mixed ligand [10-13] rhenium complexes of sulfur-containing ligands. These reactions often involve the oxidative cleavage of the rhenium-rhenium bond together with the reductive S─H, N─H or S─S bond scission in the ligands [1-6]. 2-Mercaptobenzothiazole and its derivatives are the subjects of interest in coordination and organometallic chemistry [14-24] because many of their metal complexes show antiviral, antibacterial and antifungul activity in the biological system.

This ligand may coordinate metal ions in thiol and the tautomeric thione forms as well as the deprotonated form (Chart 1). Over the last few decades, metal complexes of 2-

mercaptobenzothiazole and its derivatives, and their biological activities have been reported [14-23].

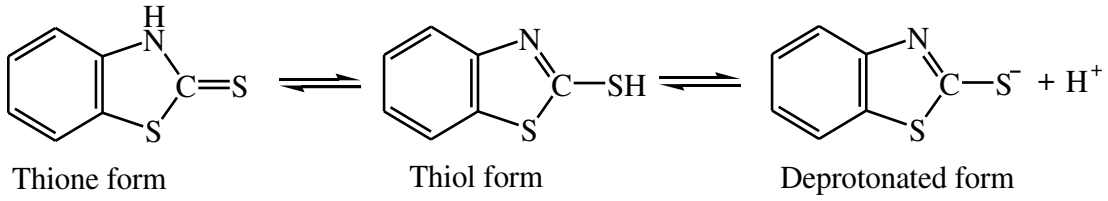

Chart 1: Different forms of 2-mercaptobenzothiazole

Derivatization of 2-mercaptobenzothiazole by inserting an alkyl group with the exocyclic sulfur atom makes a restriction of the existence of deprotonated form. Hence, the resulting system coordinates metal atoms/ions through its nitrogen atom [25] or the exocyclic sulfur atom as a two-electron donor or both nitrogen and sulfur atoms, a four-electron donor. Another coordination mode of the ligand involves the reductive carbon-sulfur bond activation in the ligand, thus acting as a six-electron donor [26]. However, the sulfur atom of the aromatic ring does not take part in coordination because its electron density is in resonance with the aromatic system (Chart 2).

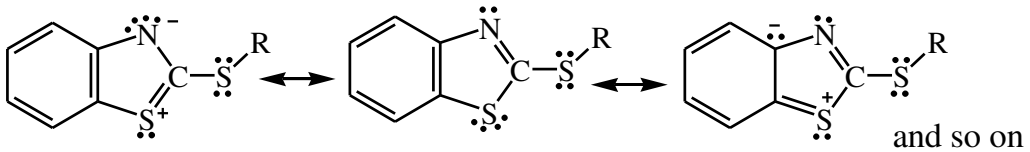

Chart 2: Resonance in 2-(alkylthio)benzothiazole (R = CH_3 and C_2H_5)

To the best of our knowledge, 2-(alkylthio)benzothiazole ligated dirhenium complexes were not reported. We have investigated the reactions of 2-(methylthio)benzothiazole and 2-(ethylthio)benzothiazole with $[Re_2(CO)_8(NCMe)_2]$, and performed DFT calculations to compare the structural properties with those of experimental X-ray crystallographic data. Besides these, we have studied the electronic properties (such as highest occupied molecular orbitals (HOMO) and lowest unoccupied molecular orbistals (LUMO) and their bandgaps) of these complexes.

Experimental

General consideration

All reactions were carried out under a dry nitrogen atmosphere. Solvents were purified and distilled from the appropriate drying agents and stored under nitrogen prior to use. Products

were separated by preparative thin layer chromatography (PTLC) on silica gel (type-60) GF_{254} Merck 7730 in air. Elemental analysis was performed by an Elementar Vario EL Cube instrument. Infrared spectra were recorded on an IR Prestige-21 FTIR spectrophotometer. NMR spectra were recorded on a Bruker Advance III HD (400 MHz) spectrometer. The precursor material, $[Re_2(CO)_8(NCMe)_2]$, was prepared according to the literature procedure [27]. 2-(Methylthio)benzothiazole and 2-(ethylthio)benzothiazole were purchased from Aldrich chemical company and used as received.

X-ray crystallography

Crystals of compounds **1** and **2** were grown from the dichloromethane solution laired by *n*-hexane. A suitable crystal was selected and mounted on a Bruker APEX3 microsource diffractometer equipped with a PHOTON II CPAD detector using a Nylon loop and Paratone oil. The crystals of compounds **1** and **2** were kept at 210.0 K during data collection using Mo-Kα radiation (λ = 0.71073). Data reduction and integration were carried out with SAINT+ program [28], and absorption corrections were applied using the program SADABS [29]. The structure was solved with the ShelXS [30] structure solution program by direct methods and refined by full-matrix least-squares on the basis of F2 using ShelXL [31] within the OLEX2 [32] graphical user interface. All non-hydrogen atoms were refined anisotropically and the hydrogen atoms were included using a riding model. Pertinent crystallographic parameters are collected in Table 1.

Table 1: Crystal data and structure refinement parameters for compound **1** and **2**

Structure parameters	**1**	**2**
Empirical formula	$C_{16}H_7NO_8Re_2S_2$	$C_{16.5}H_9NO_8Re_2S_2$
Formula weight	777.75	785.81
Temperature/K	210.0	209.99
Crystal system	triclinic	monoclinic
Space group	P-1	C2/c
a/Å	9.056	36.6989(15)
b/Å	9.469	7.0197(3)
c/Å	12.568	17.7701(7)
α/°	71.32	90
β/°	88.17	117.242(2)
γ/°	74.02	90
Volume/$Å^3$	979.6	4070.1(3)
Z	2	8

ρ_{calc}g/cm^3	2.637	2.565
μ/mm^{-1}	12.603	12.135
F(000)	712.0	2888.0
Crystal size/mm^3	0.359 × 0.322 × 0.178	0.101 × 0.088 × 0.055
Radiation	MoKα (λ = 0.71073)	MoKα (λ = 0.71073)
2Θ range for data collection/°	4.688 to 56.802	5.156 to 54.444
Index ranges	-12 ≤ h ≤ 12 -12 ≤ k ≤ 12 -16 ≤ l ≤ 16	-46 ≤ h ≤ 46 -8 ≤ k ≤ 8 -22 ≤ l ≤ 22
Reflections collected	33173	30387
Independent reflections	4869 R_{int} = 0.0730 R_{sigma} = 0.0383	4509 R_{int} = 0.0457 R_{sigma} = 0.0273
Data/restraints/parameters	4869/0/264	4509/0/274
Goodness-of-fit on F^2	1.061	1.063
Final R indexes [I>=2σ (I)]	R_1 = 0.0281, wR_2 = 0.0693	R_1 = 0.0259, wR_2 = 0.0615
Final R indexes [all data]	R_1 = 0.0323, wR_2 = 0.0713	R_1 = 0.0295, wR_2 = 0.0633
Largest diff. peak/hole / e Å^{-3}	2.30/-2.87	3.56/-1.64

DFT study

The density functional theory (DFT) calculations were executed with Gaussian16 program [33]. Initial geometries obtained from X-ray coordinates were optimized with gradient-correlated density functional theory with Becke three-parameter exchange functional [34] and the Lee-Yang-Parr functional [35] in combination with the all-electron 6-31+G(d) basis set and LanL2DZ. LanL2DZ basis set is used for heavy atom in the cluster [36]. No imaginary frequency was found for optimized structures which correspond to the true minima on the potential energy surfaces. Electronic parameters such as energy of highest occupied molecular orbital (HOMO), lowest unoccupied molecular orbital (LUMO) and band gap were calculated using the aforementioned level of theory.

Synthesis of [$Re_2(CO)_8\{\mu,\eta^1,\eta^1$-(R)$SCNSC_6H_4\}$] (1, R = CH_3, and 2, R = CH_3CH_2)

A 100 mL three-necked flask was equipped with a teflon coated magnetic stirring bar and a reflux condenser. A solution of [$Re_2(CO)_8(NCMe)_2$] (0.200 g, 0.295 mmol) and 2-(alkylthio)benzothiazole (1 eq) in freshly distilled benzene (30 mL) was refluxed for 2 hours. The color of the reaction mixture changed from yellow to orange. The solvent was removed under reduced pressure and the residue was chromatographed on silica gel TLC plates. Elution with a mixture of cyclohexane/dichloromethane (7:3 V/V) gave a slow moving major

band which resulted [$Re_2(CO)_8\{\mu,\eta^1,\eta^1$-(R)$SCNSC_6H_4\}$] (R= CH_3, 1, 0.101 g, 44%, and R = CH_3CH_2, 2, 0.093g, 40%) as orange crystals from *n*-hexane/dichloromethane mixture at 25 °C. For compound 1, found: C, 24.71; H, 0.92; N, 1.76; S, 8.20. $C_{16}H_7NO_8Re_2S_2$ requires C, 24.69; H, 0.91; N, 1.80; S, 8.23%. IR (ν_{CO} in CH_2Cl_2): 2076m, 2024s, 1978 s, br, 1950w and 1910m. ^{1}H NMR (in $CDCl_3$): δ 8.31 (1H, d, ^3J = 8.4 Hz), 7.86 (1H, d, ^3J = 8.0 Hz), 7.81 (1H, dt, ^3J = 8.0 Hz, ^4J = 0.8 Hz), 7.54 (1H, dt, ^3J = 8.0 Hz, ^4J = 0.8 Hz) and 3.22 (3H, s, Me). For compound 2 found: C, 25.78; H, 1.16; N, 1.75; S, 8.06. $C_{17}H_9NO_8Re_2S_2$ requires C, 25.76; H, 1.15; N, 1.76; S, 8.08%. IR (ν_{CO} in CH_2Cl_2): 2076m, 2024s, 1978s,br, 1950w and 1909m. ^{1}H NMR (in $CDCl_3$): δ 8.29 (1H, d, ^3J = 8.8 Hz), 7.84 (1H, d, ^3J = 8.0 Hz), 7.79 (1H, dt, ^3J = 8.4 Hz, ^4J = 0.4 Hz), 7.51 (1H, dt, ^3J = 8.0 Hz, ^4J = 0.4 Hz), 3.35 (2H, q, ^3J = 8.20 Hz) and 1.54 (3H, t, ^3J = 8.20 Hz).

Results and discussion

Synthesis and spectroscopic characterization of 1 and 2

The equimolar reaction between the labile complex, [$Re_2(CO)_8(NCMe)_2$], with 2-(methylthio)benzothiazole and 2-(ethylthio)benzothiazole at 80 °C followed by chromatographic separation resulted the products [$Re_2(CO)_8\{\mu,\eta^1,\eta^1$-($CH_3$)$SCNSC_6H_4\}$] (**1**, 44%) and [$Re_2(CO)_8\{\mu,\eta^1,\eta^1$-($C_2H_5$)$SCNSC_6H_4\}$] (**2**, 40%), respectively as orange crystals (Scheme 1). The complexes gave satisfactory results in elemental analysis consistent with their structures. The solution (in CH_2Cl_2) phase IR spectrum of compound **1** shows bands at 2076m, 2024s, 1978s,br, 1950w and 1910m in its carbonyl stretching region indicating that all carbonyl groups are terminally coordinated [37]. The carbonyl stretching region of the IR spectrum of compound **2** shows very similar pattern (2076m, 2024s, 1978s,br, 1950w and 1909m). The ^{1}H NMR spectrum of compound **1** shows signals at δ3.22 (3H, s, Me) in aliphatic region for the SCH_3 group and δ 8.31 (1H, d, ^3J = 8.4 Hz), 7.86 (1H, d, ^3J = 8.0 Hz), 7.81 (1H, dt, ^3J = 8.0 Hz, ^4J = 0.8 Hz) and 7.54 (1H, dt, ^3J = 8.0 Hz, ^4J = 0.8 Hz) for the aromatic protons. The ^{1}H NMR spectrum of compound **2** shows signals at δ3.35 (2H, q, ^3J = 8.20 Hz) and δ1.54 (3H, t, ^3J = 8.20 Hz) for SCH_2CH_3 group, and δ 8.29 (1H, d, ^3J = 8.8 Hz), 7.84 (1H, d, ^3J = 8.0 Hz), 7.79 (1H, dt, ^3J = 8.4 Hz, ^4J = 0.4 Hz) and 7.51 (1H, dt, ^3J = 8.0 Hz, ^4J = 0.4 Hz) for the aromatic protons.

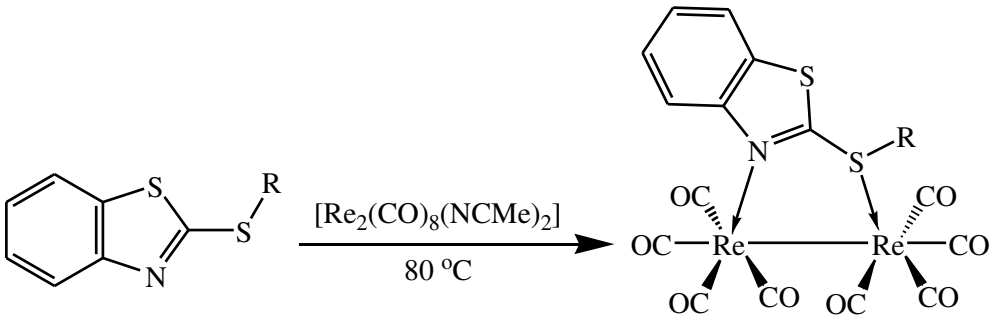

1 : R = CH_3

2 : R = CH_2CH_3

Scheme 1: Synthesis of $[Re_2(CO)_8\{\mu,\eta^1,\eta^1\text{-}(R)SCNSC_6H_4\}]$ (**1**, R = CH_3 and **2**, R = CH_3CH_2)

Crystallographic characterization of 1 and 2

Crystals of compounds **1** and **2** were grown from the dichloromethane solution of the compounds laired with *n*-hexane by the laired diffusion method. Suitable-sized crystals were chosen for diffraction analysis. The molecular structures of compounds **1** and **2** are shown in Figure 1 and Figure 2, respectively. Selected matrices of compounds **1** and **2** were compared with their calculated values in Table 1 and Table 2, respectively. Compounds **1** and **2** have structural similarities, but their crystal systems are different. Compound **1** crystallized as a triclinic crystal system with *P*-1 space group, but compound **2** crystallized as a monoclinic crystal system with the space group *C2/c*, and their unit cells are centrosymmetric possessing an inversion center.

The rhenium-rhenium bond distance of 2.9735(2) Å and 2.9925(3) Å in compounds **1** and **2**, respectively, clearly corresponds to a rhenium-rhenium single bond, which is in accordance with the 18-electron count for each metal atom. The rhenium-rhenium single bond distances in compounds **1** and **2** are shorter than the reported dirhenium compounds [38-52]. The ligation of 2-(alkylthio)benzothiazole to the dirhenium core through the nitrogen and sulfur atoms of the ligand results a five-membered metallacycle which does not allow the rhenium-rhenium bond to relax, and hence a significant shortening of the rhenium-rhenium bond in **1**. The rhenium-rhenium bond distance in compounds **1** and **2** are in the comparable range, [2.9578(4) Å – 2.9873(3) Å], in reported five-membered metallacycles [53].

The observed rhenium-nitrogen bond distance in compounds **1** and **2** are 2.236(4) Å and 2.225(4) Å, respectively are within the range of the reported rhenium-nitrogen bond distances [1,3,4,6-13,19,46,48-51,53-61]. To the best of our knowledge, the longest rhenium-nitrogen single bond [2.292(7) Å] was reported in *fac*–$[ReCl(CO)_3(quinox)]$ [59], [quinox = 2-(4,5-

dihydro-2-oxazolyl)quinolone], and the shortest rhenium-nitrogen single bond [2.090(5) Å] is reported in $[Re_2(\mu\text{-mp})_4Cl_2].2C_6H_6$ [61].

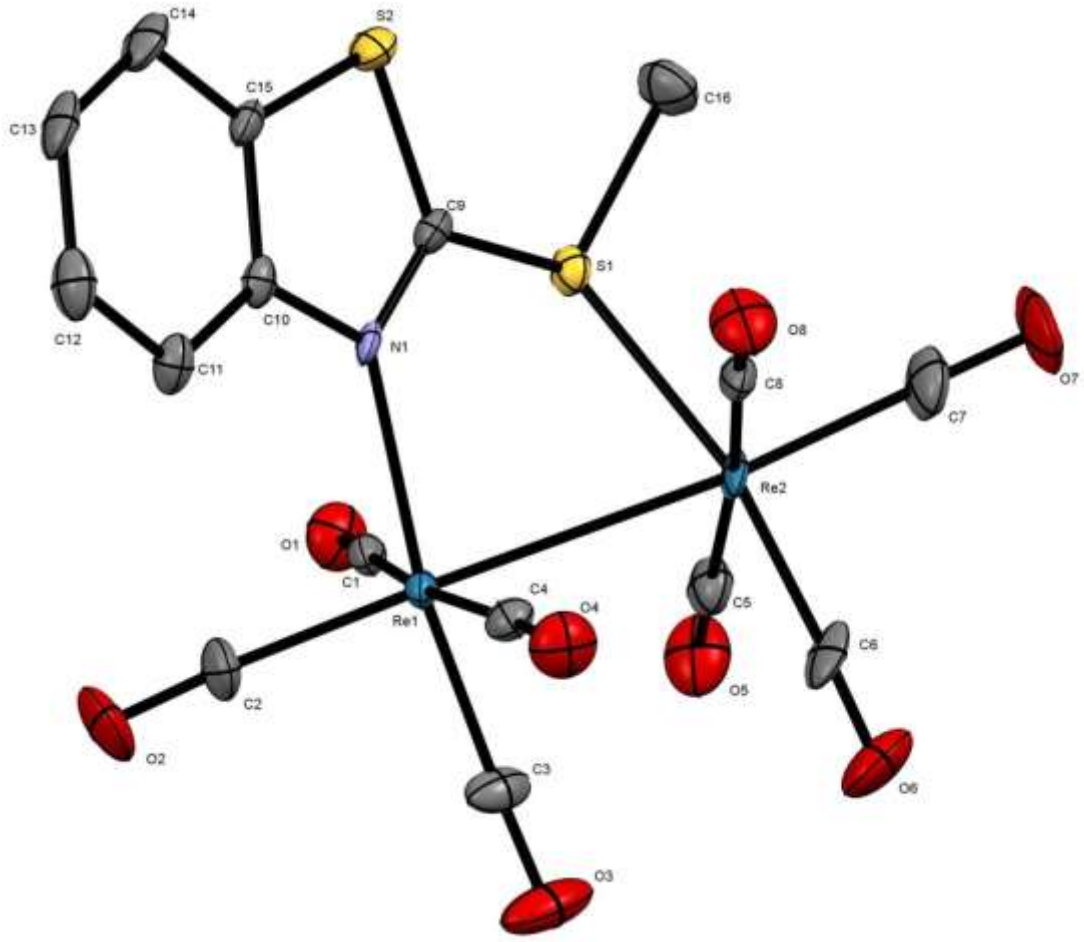

Figure 1: Solid-state molecular structure of $[Re_2(CO)_8\{\mu,\eta^1,\eta^1\text{-}(CH_3)SCNSC_6H_4\}]$ (**1**). The atomic displacement ellipsoids are drawn at the 50% probability, and hydrogen atoms are omitted for clarity.

The observed rhenium-sulfur bond distances in compounds **1** and **2** are 2.4358(11) Å and 2.4554(13) Å, respectively shorter than the reported complexes [1,3,4,6,7,9,10,12,13,39,41,54,56,57]. However, the rhenium-sulfur bond distances in compounds **1** and **2** are comparable to the rhenium-sulfur bond distances [2.4493(11) Å – 2.4632(11) Å] reported in five-membered metallahetrocycles [53]. The Re−N bond of **1** is somewhat longer than that of **2**, but the opposite phenomenon is observed for their Re−S bonds. The bulkier ethyl group of 2-(ethylthio)benzothiazole ligand in **2** causes a significant tilt of the ligand, supporting the longer Re−S and shorter Re−N bond distances.

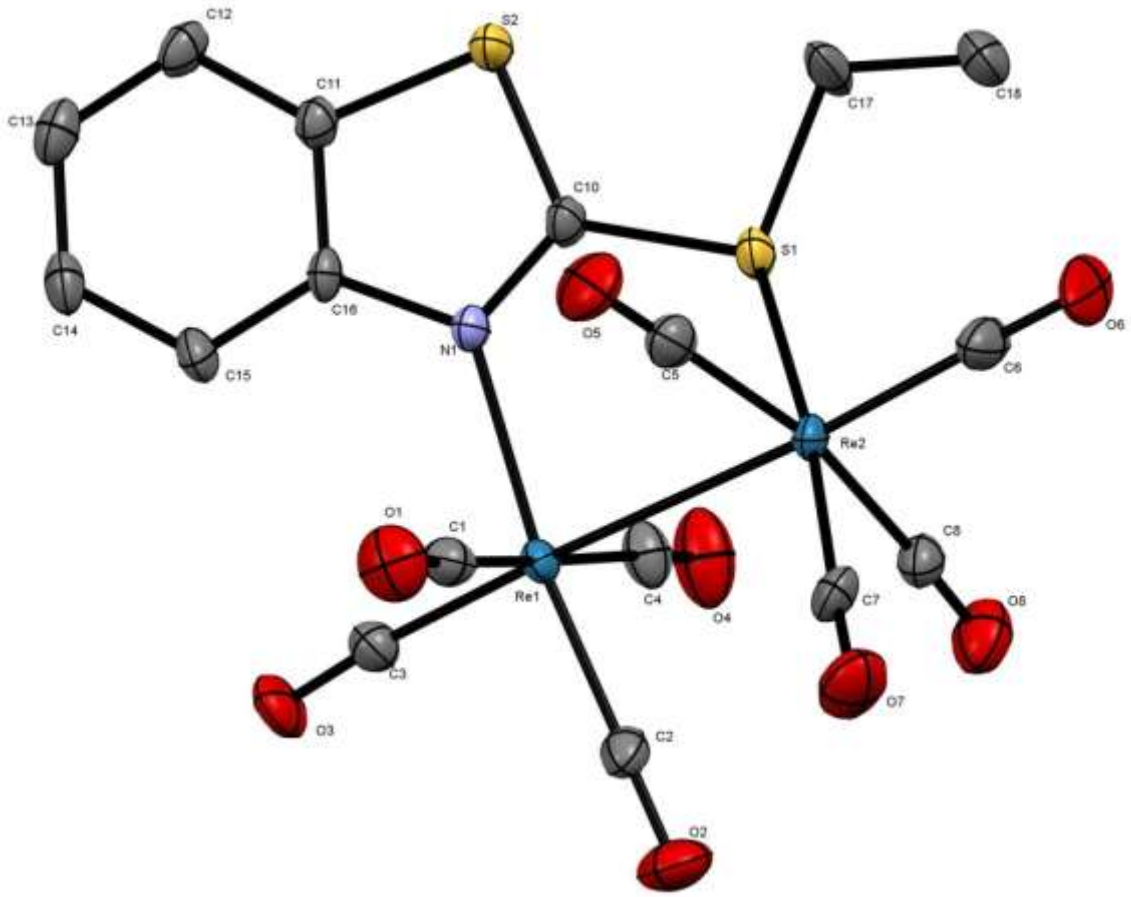

Figure 2: Solid state molecular structure of $[Re_2(CO)_8\{\mu,\eta^1,\eta^1\text{-}(C_2H_5)SCNSC_6H_4\}]$ (**2**). The atomic displacement ellipsoids are drawn at the 50% probability, and hydrogen atoms are omitted for clarity.

Both compounds consist of a dirhenium core coordinated with eight terminal carbonyl ligands and a 2-(alkylthio)benzothiazole ligand acting as four-electron donor. An interesting structural feature of the compounds is the coordination of 2-(alkylthio)benzothiazole ligand in a μ,η^1,η^1- fashion, one rhenium atom through the nitrogen atom and the other rhenium atom through the sulfur atom without scission of the rhenium-rhenium and carbon-sulfur bond. So the ligation of the 2-(alkylthio)benzothiazole ligand does not affect the structural integrity of the dirhenium core and the ligand framework. The structure of the compounds is better discussed by two square pyramidal units joining together with a rhenium-rhenium bond; thus each rhenium core is in an octahedral coordination sphere supported by the bond angles about each rhenium cores. The Re1 atom of both compounds is coordinated with four carbonyl groups, the nitrogen atom of 2-(alkylthio)benzothiazole ligand and one neighboring rhenium atom. The Re2 atom is coordinated with four carbonyl groups, the exocyclic sulfur atom of the 2-(alkylthio)benzothiazole ligand and Re1 atom. In compounds 1 and 2, the 2-

(alkylthio)benzothiazole ligand coordinates the two rhenium atoms from the equatorial position.

Table 1: Selected calculated and experimental matrices of $[Re_2(CO)_8\{\mu,\eta^1,\eta^1\text{-}(CH_3)SCNSC_6H_4\}]$ (**1**)

Matrix description	DFT calculated matrices (Å,°)	Experimental matrices (Å,°)
Re1-Re2	3.068	2.9735(2)
Re1-C1^{e}	1.984	1.986(5)
Re1-C2^{a}	1.926	1.928(5)
Re1-C3$^{e,¤}$	1.929	1.934(5)
Re1-C4^{e}	1.986	1.993(4)
Re2-C5^{e}	1.989	2.000(5)
Re2-C6^{e,§}	1.924	1.930(5)
Re2-C7^{a}	1.929	1.927(5)
Re2-C8^{e}	1.975	1.973(5)
O1-C1^{e}	1.175	1.136(6)
O2-C2^{a}	1.182	1.127(6)
O3-C3$^{e,¤}$	1.177	1.132(6)
O4-C4^{e}	1.175	1.128(5)
O5-C5^{e}	1.174	1.140(6)
O6-C6^{e,§}	1.177	1.149(6)
O7-C7^{a}	1.182	1.122(6)
O8-C8^{e}	1.177	1.148(6)
Re1-N1	2.281	2.236(3)
Re2-S1	2.58	2.4358(11)
N1-Re1-Re2	85.2	84.83(9)
S1-Re2-Re1	76.9	77.29(3)
C2-Re1-N1	95.7	96.94(19)
C7-Re2-S1	94.5	96.81(18)

'a' axial, 'e' equatorial, '¤' *anti* to N-atom, and '§' *anti* to S-atom

The Re─C(axial) bond distances [1.928(5) and 1.927(5) Å in **1**, and 1.918(5) and 1.922(6) Å in **2**] are somewhat shorter than the Re─C(equatorial) bond distances [1.986(5), 1.934(5), 1.993(4), 2.000(5), 1.930(5) and 1.973(5) Å in **1**, and 1.996(6), 1.928(5), 1.983(6), 1.957(6), 1.927(6) and 1.997(5) Å in **2**] which is compatible with the parent complex, $Re_2(CO)_{10}$ [38]. Two equatorial CO ligands *anti* to each other cause a significant restriction to donate their electron density to the metal core, which results a less back donation and hence weakening the Re–C bonds. The average Re─C bond distance of compounds **1** and **2** are 1.959 and 1.954 Å, respectively are remarkably shorter than the average Re─C bond distance (1.975 Å)

in the parent compound, $Re_2(CO)_{10}$ [38]. This is due to the stronger electron-donating capacity of the 2-(alkylthio)benzothiazole ligand than CO, which results a significant electron back donation, thus strengthening the Re─C bonds. This phenomenon is further supported by the longer average C─O bond distances (1.135 Å in **1** and 1.139 Å in **2**) compared to that of $Re_2(CO)_{10}$ [1.132 Å] [38]. The insertion of the 2-(alkylthio)benzothiazole ligand results the equatorial CO ligands to divide into two subgroups, based on the Re─C bond distances. The carbonyl groups *anti* to the N- or S- atom of the ligand are facing more electron back donation and hence result two shorter $Re─C_{equatorial}$ [1.934(5) and 1.930(5) Å in **1**, and 1.928(5) and 1.927(6) Å in **2**] than the other four $Re─C_{equatorial}$ bond distances.

Table 2: Selected calculated and experimental matrices of $[Re_2(CO)_8\{\mu,\eta^1,\eta^1\text{-}(C_2H_5)SCNSC_6H_4\}]$ (**2**)

Matrix Description	DFT calculated matrices (Å,°)	Experimental matrices (Å,°)
Re1-Re2	3.069	2.9925(3)
Re1-C1^{e}	1.986	1.996(6)
Re1-C2$^{e,¤}$	1.929	1.928(5)
Re1-C3^{a}	1.927	1.918(5)
Re1-C4^{e}	1.984	1.983(6)
Re2-C5^{e}	1.975	1.957(6)
Re2-C6^{a}	1.927	1.922(6)
Re2-C7^{e,§}	1.922	1.927(6)
Re2-C8^{e}	1.988	1.997(5)
O1-C1^{e}	1.175	1.135(7)
O2-C2$^{e,¤}$	1.177	1.140(7)
O3-C3^{a}	1.182	1.145(7)
O4-C4^{e}	1.175	1.131(7)
O5-C5^{e}	1.177	1.148(7)
O6-C6^{a}	1.182	1.148(7)
O7-C7^{e,§}	1.177	1.141(7)
O8-C8^{e}	1.174	1.123(7)
Re1-N1	2.278	2.225(4)
Re2-S1	2.592	2.4554(13)
N1-Re1-Re2	84.8	85.47(10)
S1-Re2-Re1	76.6	77.73(3)
C3-Re1-N1	95.5	96.34(19)
C6-Re2-S1	97.0	97.18(19)

'a' axial, 'e' equatorial, '¤' *anti* to N-atom, and '§' *anti* to S-atom

The Re atoms of the compounds are in the octahedral coordination sphere, but the bond angles about the Re cores suggest there is a profound distortion from the ideal octahedral geometry. The observed N1—Re1—Re2 and S1—Re2—Re1 bond angles in compound **1** are 84.83(9) and 77.29(3)°, respectively, which is due to the rigid structure of the ligating 2-(methylthio)benzothiazole ligand. The C2—Re1—N1 and C7—Re2—S1 bond angles are 96.94(19) and 96.81(18)°, respectively, supporting that the bulky 2-(methylthio)benzothiazole ligand exerts a force to the axial CO ligands resulting a notable extent of distortion. Compound **2** displays a similar phenomenon where the angles of N1—Re1—Re2, S1—Re2—Re1, C3—Re1—N1, and C6—Re2—S1 are 85.47(10), 77.73(3), 96.34(19), and 97.18(19)°, respectively.

The 2-(alkylthio)benzothiazole ligand is almost perpendicular to the Re−Re vector of the complexes, but the coordinating nitrogen and exocyclic sulfur atoms are not coplanar. The observed S−Re−Re−N dihedral angle in compounds **1** and **2** are 37.36° and 34.88°, respectively (Chart 3).

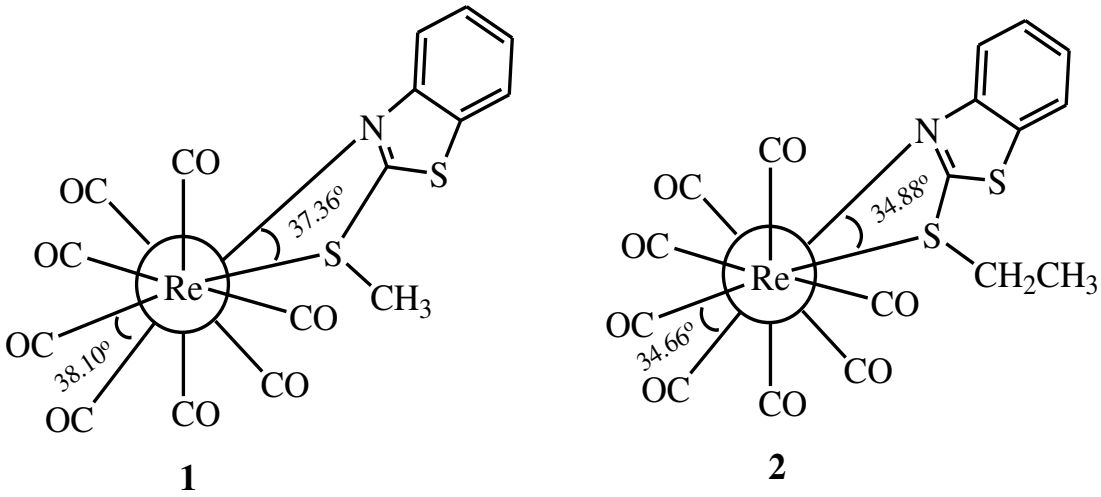

Chart 3: Newman projection formula for compounds **1** and **2** showing notable dihedral angles

DFT study

Initial geometries taken from X-ray refinement data was optimized as a free molecule in vacuum state. The properties of optimized geometries such as bond lengths and angles are compared with experimental values (Tables 1 and 2). They are in good agreement with experimental data except for few values. The maximum deviation between simulated and experimental bond lengths are observed for Re—S bonds in both complexes (0.1442 Å in **1**

and 0.1366 Å in **2**). The maximum deviations between calculated and experimental bond angles in compounds **1** and **2** are 3.65° and 4.16°, respectively. However, these deviations are expected because compounds **1** and **2** belong to the isolated molecules in vacuum during optimization, but experimental results belong to the temperature effect, intermolecular interactions, and crystal packing effect.

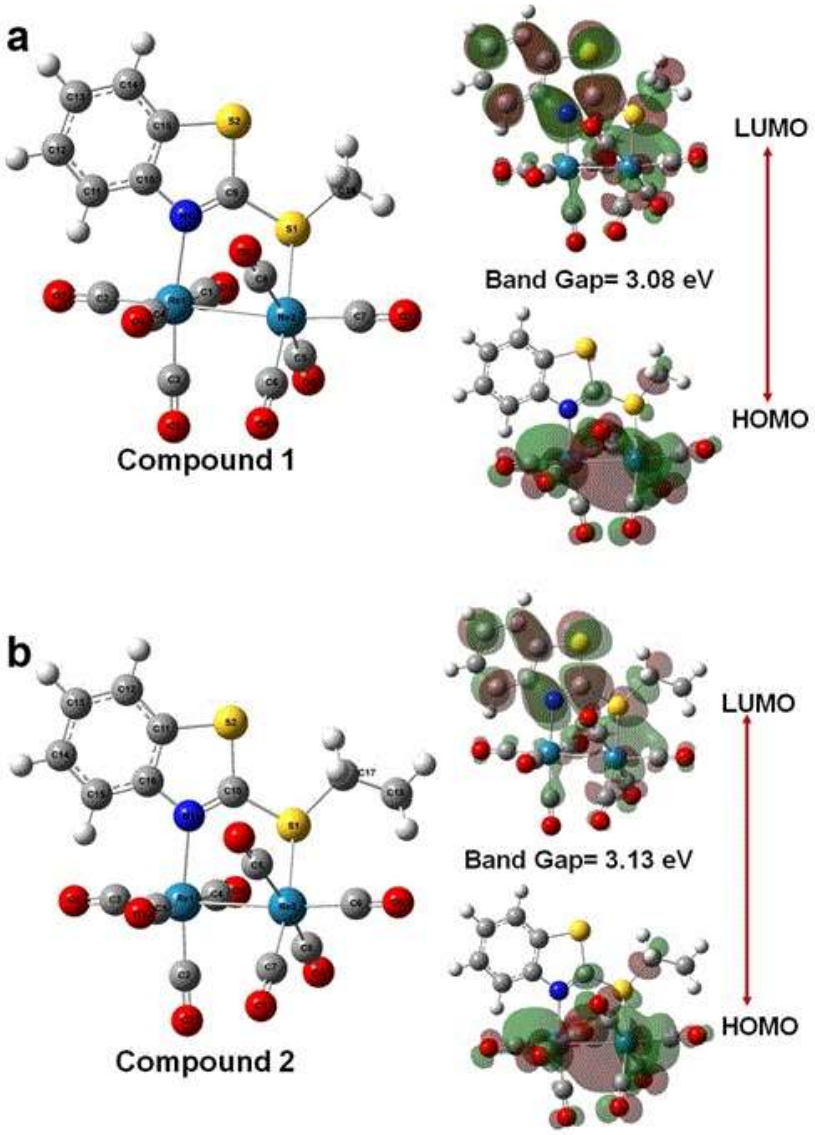

Figure 3: Optimized structures and calculated frontier molecular orbitals of (a) compound **1** and (b) compound **2**

The electronic and optical properties of a compound can be explained based on its Frontier Molecular Orbitals (FMOs), i. e. HOMO (highest occupied molecular orbital) and LUMO (lowest unoccupied molecular orbital). The energy difference between HOMO and LUMO is defined as bandgap is an important parameter to determine the stability of the structure. The

calculated energies of HOMO and LUMO of compound **1** (compound **2**) are -5.87 (-5.84) eV and -2.79 (-2.71) eV (Figure 3). For both compounds, HOMO is distributed on $Re_2(CO)_8$ while LUMO is mainly delocalized on 2-(alkylthio)benzothiazole ligand. The band gaps for compounds **1** and **2** are 3.08 eV and 3.13 eV, respectively. Compound **2** has 0.05 eV larger bandgap than compound **1**. These values of bandgap generally classify the compounds as semiconductors which have application in photovoltaics and optoelectronics [62]. However, the semiconducting properties of the complexes will be studied later, and the results will be published elsewhere. The calculated hardness and softness of compound **1** (compound **2**) are 1.54 (1.57) eV and 0.32 (0.32) eV, respectively. The compounds have a large hardness value and a small softness value, which indicate that compounds are prone to chemical reactions [63].

Hirshfeld surface analysis: Crystal Explorer 17.5 has been used to perform Hirshfeld surface analysis which quantifies the intermolecular interaction and identifies the close contact atoms in a molecular crystal. The Hirshfeld surface of a molecular crystal is mapped over d_{norm} which is defined by the following expression;

$$d_{norm} = \frac{d_i - r_i^{vdW}}{r_i^{vdW}} + \frac{d_e - r_e^{vdW}}{r_e^{vdW}}$$

where d_e and d_i are distances from a point on the surface to the nearest nucleus outside the surface and inside the surface, respectively. r_i^{vdW} and r_i^{vdW} are the van der Waals radii of the atoms those lie inside and outside the Hirshfeld surface, respectively. The Hirshfeld surface mapped over d_{norm} of compounds **1** and **2** are illustrated in Figure 4. The color gradient in these figures varies from red (negative d_{norm} value) through white (d_{norm} value of zero) to blue (positive d_{norm} value).

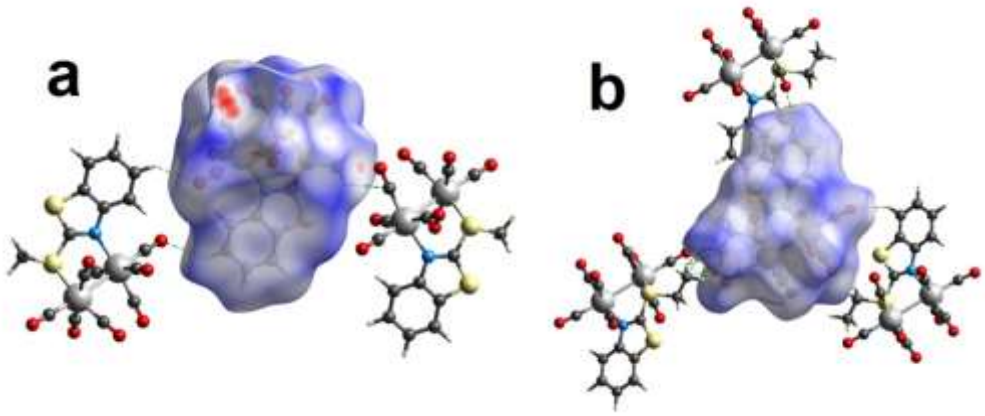

Figure 4: Perspective view of the d_{norm} Hirshfeld surfaces of (a) compound **1** and (b) compound **2**

The Hirshfeld surface of compound **1** was generated with the d_{norm} surface mapped over a fixed color scale of -0.1319 Å (red) to 1.2641 Å (blue) and for compound **2** -0.4436 Å (red) to 1.4136 Å (blue). The red circular spots over the Hirshfeld surface indicate the strong O---H and C---H hydrogen bond interactions (Figures 4a and 4b). Here, the O---H contact is one of the prominent contacts which is significant in crystal packing for both compounds. This is evident in the 2D fingerprint plots (Figures 5 and 6).

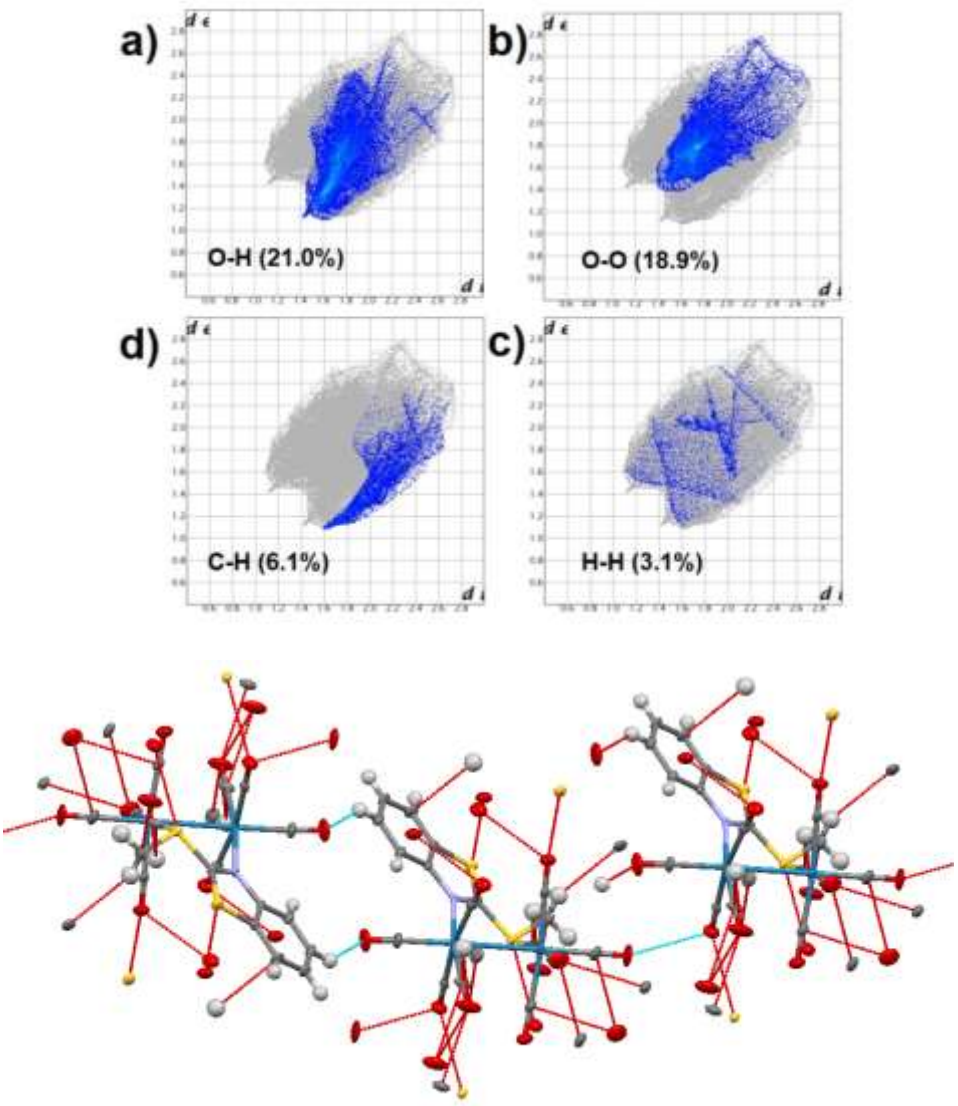

Figure 5: 2D fingerprint plots showing the main close contact contributions (%) for a) O---H, b) O---O, c) H---H and d) C---H on the Hirshfeld surface area (top), and observed close contact (bottom) for compound **1**.

Significant intermolecular interactions, which are mapped in Figure 5 and Figure 6, show the largest contribution of the H---O interaction in compound **1** (compound **2**) 21.0% (21.5%) with a sharp spike (d_e+d_i ~ 2.5 Å (2.4 Å)). This spike indicates the strong hydrogen bond

interaction. Another significant contribution in the two compounds is O---O contacts which are 18.9% in compound **1** and 18.4% in compound **2** of the Hirshfeld area. However, this contact is not visible as a red spot on the Hirshfeld surface. All other contacts observed are C---H and H---H, which contribute to compound **1** (compound **2**) 6.1% (6.1%) and 3.1% (5.5%). Therefore, it is clear that H---O and O---O contacts are significant in the packing arrangement of both crystals. Bottom figures in 5 and 6 show the observed intermolecular interactions responsible for the packing arrangement and formation of the three-dimensional crystals of compounds **1** and **2**, respectively, found from the X-ray crystallographic study, which are consistent with the theoretical analysis.

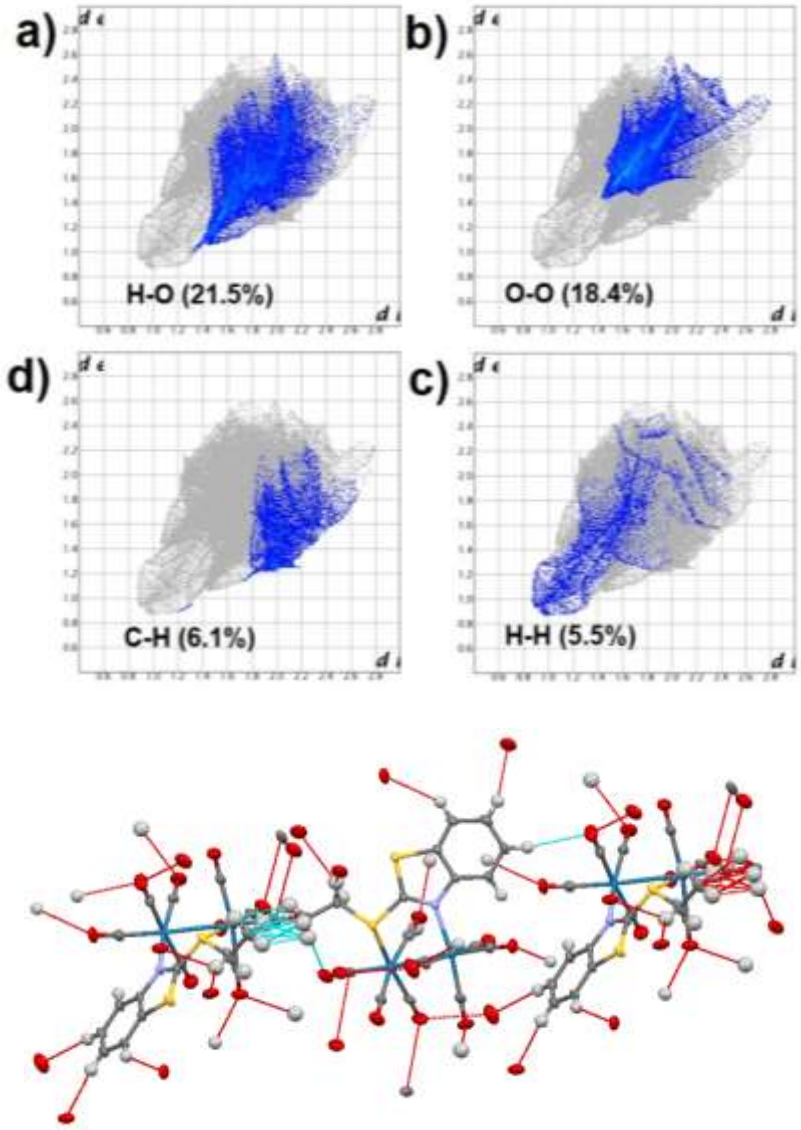

Figure 6: 2D fingerprint plots showing the main close contact contributions (%) for a) O---H, b) O---O, c) H---H and d) C---H on the Hirshfeld surface area (top), and observed close contact (bottom) for compound **2**.

Conclusions

Two novel dirhenium complexes having the general formula, $[Re_2(CO)_8\{\mu,\eta^1,\eta^1\text{-}(R)SCNSC_6H_4\}]$ (R = CH_3 and CH_2CH_3) were synthesized and structurally characterized. The structures of the complexes were optimized with the help of DFT method, and the calculated bond lengths and bond angles are found in good agreement with the X-ray crystallographic data. The energy gaps between HOMO and LUMO were found 3.08 (for methyl derivative) and 3.13 eV (for the ethyl analog) supporting the semiconducting properties of the complexes. Intermolecular interaction, crystal packing as well as identification of close contact in the complexes were studied with the help of Hirshfeld surface analysis, and O---H interaction is found as the most dominant inter contact (21.0% in **1** and 21.5% in **2**) in crystal packing of the complexes.

Funding

Not Applicable.

Conflict of interest

The authors declare that they have no competing interest that could have appeared to influence the work reported in this paper.

Availability of data and materials

Crystallographic data for the structural analysis of the compounds have been deposited to the Cambridge Crystallographic Data Centre. These data may be obtained free of charge from The Director, Cambridge Crystallographic Database Centre, 12 Union Road Cambridge, CB2 1EZ, United Kingdom. (http://www.ccdc.cam.ac.uk).

Code Availability

CCDC 1976501 for compound **1** and CCDC 1976360 for compound **2**.

Author's Contribution

Laboratory work was carried out by MWI under the supervision of MMK and SI. X-ray crystallography was done by NCB, and JKS did the theoretical calculation. The draft manuscript was prepared by SI. All authors contributed to edit the manuscript except MMK

since he passed away while the research work was in progress. The final version of the manuscript was approved by all authors.

Acknowledgements

We acknowledge Ministry of Science and Technology, Government of the People's Republic of Bangladesh for financial support, and Md. Emdad Hosen, Scientist, Wazed Miah Science Research Center, Jahangirnagar University, for performing elemental analysis as well as for recording IR and NMR spectra of the sample.

References

1. Deeming AJ, Karim M, Bates PA, Hursthouse MB (1988) A new type of pyridine-2-thionato bridge: X-ray crystal structure of the complex $[Re_2(MepyS)_2(CO)_6]$ where MepyS is the 6-methylpyridine-2-thionato ligand. Polyhedron 7:1401–1403. https://doi.org/10.1016/S0277-5387(00)80393-9

2. Hossain MI, Ghosh S, Hogarth G, Kabir SE (2013) Reactions of $M_2(CO)_9L$ (M = Re, Mn; L = CO, MeCN) with thioacetamide and thiobenzamide: Facile metal-mediated nitrogen-hydrogen bond activation and subsequent carbon-nitrogen or sulfur-sulfur bond formation. J Organomet Chem 737:53–58. https://doi.org/10.1016/j.jorganchem.2013.03.011

3. Vanitha A, Sathiya P, Sangilipandi S, et al (2010) One-pot synthesis of sulphur bridged dinuclear rhenium metallacycles via addition of S-S bond across Re-Re bond. J Organomet Chem 695:1458–1463. https://doi.org/10.1016/j.jorganchem.2010.02.027

4. Kabir SE, Alam J, Ghosh S, et al (2009) Synthesis, structure and reactivity of tetranuclear square-type complexes of rhenium and manganese bearing pyrimidine-2-thiolate (pymS) ligands: Versatile and efficient precursors for mono- and polynuclear compounds containing $M(CO)_3$ (M = Re, Mn) fragment. J Chem Soc Dalt Trans 4458–4467. https://doi.org/10.1039/b815337j

5. Hoque MA, Miah MA, Abser MN, et al (2012) Binuclear Rhenium and Manganese Carbonyl Compounds Containing Hetero-Mercaptanes. J Bangladesh Chem Soc 25:62–70. https://doi.org/10.3329/jbcs.v25i1.11775

6. Hoque A, Islam S, Karim M, et al (2015) Variations in binding modes of 2-mercaptobenzoxazolates in the novel cyclic trinuclear complexes $[Mn_3(CO)_{10}(\mu$-

$SCNOC_6H_4)_3$] and [$Re_3(CO)_{12}$(μ-$SCNOC_6H_4)_3$]. Inorg Chem Commun 54:69–72. https://doi.org/10.1016/j.inoche.2015.02.008

7. Ahmad MF, Sarker JC, Azam KA, et al (2013) $Re_2(CO)_6$(μ-thpymS)$_2$ (thpymSH = pyrimidine-2-thiol) as a versatile precursor to mono- and polynuclear complexes: X-ray crystal structures of fac-$Re(CO)_3(PPh_3)$ (κ^2-thpymS) and two isomers of $ReRu_3(CO)_{13}$(μ_3-thpymS). J Organomet Chem 728:30–37. https://doi.org/10.1016/j.jorganchem.2012.12.030

8. Moni MR, Mia MJ, Ghosh S, et al (2018) Investigation on the reactivity of tetranuclear Group 7/8 mixed-metal clusters toward triphenylphosphine. Polyhedron 146:154–160. https://doi.org/10.1016/j.poly.2018.02.026

9. Moni MR, Ghosh S, Mobin SM, et al (2018) Diphosphine-induced thiolate-bridge scission of [$Re(CO)_3$(μ,κ^2-S,N-thpymS)]$_2$ (thpymS = 1,4,5,6-tetrahydropyrimidine-2-thiolate): Structural and computational studies of configurational isomers of [$Re(CO)_3$(κ^2-S,N-thpymS)]$_2$(μ,κ^1,κ^1-dppe). J Organomet Chem 871:167–177. https://doi.org/10.1016/j.jorganchem.2018.07.005

10. Nkoe PI, Visser HG, Swart C, et al (2018) Synthesis of re1tricarbonyl complexes with various sulfur-and oxygen-donating ligands: Crystal structures of two re1dinuclear structures bridged by S atoms. Acta Crystallogr Sect C Struct Chem 74:1116–1122. https://doi.org/10.1107/S205322961801207X

11. Veronese L, Quartapelle Procopio E, Maggioni D, et al (2017) Dinuclear rhenium pyridazine complexes containing bridging chalcogenide anions: Synthesis, characterization and computational study. New J Chem 41:11268–11279. https://doi.org/10.1039/c7nj02548c

12. Nkoe PI, Koen R, Brink A, Schutte-Smith M (2016) Crystal structure of hexacarbonyl bis(μ_2-2-methoxybenzenethiolato-κ2S)pyridine(triphenylphosphane)dirhenium(I), $C_{43}H_{34}NO_8PS_2Re_2$. Zeitschrift fur Krist - New Cryst Struct 231:461–464. https://doi.org/10.1515/ncrs-2015-0139

13. Karthikeyan M, Govindarajan R, Duraisamy E, et al (2017) Self-Assembly of Chalcogenolato-Bridged Ester and Amide Functionalized Dinuclear Re(I) Metallacycles: Synthesis, Structural Characterization and Preliminary Cytotoxicity Studies. ChemistrySelect 2:3362–3368. https://doi.org/10.1002/slct.201700646

14. El-Shazly MF, Salem T, El-Sayed MA, Hedewy S (1978) Coordination chemistry of benzothiazole derivatives. 2-mercaptobenzothiazole and 2-(o-hydroxyphenyl)benzothiazole complexes with Cu(II), Ni(II) and Co(II). Inorganica Chim Acta 29:155–163. https://doi.org/10.1016/S0020-1693(00)89641-3

15. Banerji S, Byrne RE, Livingstone SE (1982) Metal complexes of 2-mercaptobenzothiazole. Transit Met Chem 7:5–10. https://doi.org/10.1007/BF00623797

16. Hussein A, Devillanova FA, Isaia F, Verani G (1985) Copper(I) complexes withN-methylbenzothiazole-2-thione and -2-selone. Transit Met Chem 10:368–370. https://doi.org/10.1007/BF00618844

17. Loeb B, Crivelli I, Andrade C (1991) The 2-Mercaptobenzothiazole and Copper(II) Reaction. Synth React Inorg Met Chem 21:331–342. https://doi.org/10.1080/15533179108020186

18. Khan TA, Shahjahan (1998) Biheterocyclic ligands. Transition metal complexes of 2-(1-pyridine-2-thionato)benzoxazole and 2-(1-pyridine-2-thionato)benzothiazole - synthesis and characterization. Synth React Inorg Met Chem 28:571–586. https://doi.org/10.1080/00945719809351666

19. Akrivos PD (2001) Recent studies in the coordination chemistry of heterocyclic thiones and thionates. Coord Chem Rev 213:181–210. https://doi.org/10.1016/S0010-8545(00)00372-6

20. Tsiaggali MA, Andreadou EG, Hatzidimitriou AG, et al (2013) Copper(I) halide complexes of N-methylbenzothiazole-2-thione: Synthesis, structure, luminescence, antibacterial activity and interaction with DNA. J Inorg Biochem 121:121–128. https://doi.org/10.1016/j.jinorgbio.2013.01.001

21. Aslanidis P, Hatzidimitriou AG, Andreadou EG, et al (2015) Silver(I) complexes of N-methylbenzothiazole-2-thione: Synthesis, structures and antibacterial activity. Mater Sci Eng C 50:187–193. https://doi.org/10.1016/j.msec.2015.02.014

22. Varna D, Psomas G, Choli-Papadopoulou T, et al (2016) Dinuclear copper(I) complexes of N-methylbenzothiazole-2-thione: synthesis, structures, antibacterial activity and DNA interaction. J Coord Chem 69:2500–2513. https://doi.org/10.1080/00958972.2016.1206893

23. Ahmed AJ, Ali Alsammarraie AM (2018) Synthesis, Spectral, Structural and Antimicrobial Studies of Silver Nanoparticles and Ag(I) Complex of 2-Mercaptobenzothiazole. Asian J Chem 30:1608–1612. https://doi.org/10.14233/ajchem.2018.21291

24. Ghosh S, Alam Mia MS, Begum E, et al (2012) Synthesis, structure and reactivity of $[Mn_2(CO)_6(\mu\text{-MBT})_2]$ (MBT = 2-mercaptobenzothiazolato): A versatile precursor for mono- and polynuclear compounds. Inorganica Chim Acta 384:76–82. https://doi.org/10.1016/j.ica.2011.11.035

25. Miah JA (2017) Studies on the reaction of Gr-VIII Transition Metals with Mercaptane Ligands. Unpublished PhD Work, Dept Chem Jahangirnagar Univ Savar, Dhaka-1342, Bangladesh.

26. Sohel KM (2013) Studies on Some Complexes of Group VII and VIII Transition Metal Carbonyls Bearing Sulfur, Nitrogen and Oxygen Donor Simple Molecules. Unpublished PhD Work, Dept Chem Jahangirnagar Univ Savar, Dhaka-1342, Bangladesh.

27. Bruce MI, Low PJ (1996) Expeditious synthesis of $Re_3(\mu\text{-H})_3(CO)_{11}(NCMe)$. J Organomet Chem 519:221–222. https://doi.org/10.1016/S0022-328X(96)06231-6

28. Bruker (2015) SAINT (8.37A), Bruker AXS Inc., Madison, Wisconsin, USA.

29. Bruker (2014) SADABS-2014/5, Bruker AXS Inc., Madison, Wisconsin, USA.

30. Sheldrick GM (2008) A short history of SHELX. Acta Crystallogr Sect A A64:112–122. https://doi.org/10.1107/S0108767307043930

31. Sheldrick GM (2015) Crystal structure refinement with SHELXL. Acta Crystallogr Sect C Struct Chem C71:3–8. https://doi.org/10.1107/S2053229614024218

32. Dolomanov OV, Bourhis LJ, Gildea RJ, et al (2009) OLEX2 : a complete structure solution, refinement and analysis program. J Appl Crystallogr 42:339–341. https://doi.org/10.1107/S0021889808042726

33. Schmidt MW, Baldridge KK, Boatz JA, et al (1993) General atomic and molecular electronic structure system. J Comput Chem 14:1347–1363. https://doi.org/10.1002/jcc.540141112

34. Becke AD (1993) Density-functional thermochemistry. III. The role of exact

exchange. J Chem Phys 98:5648–5652. https://doi.org/10.1063/1.464913

35. Lee C, Yang W, Parr RG (1988) Development of the Colle-Salvetti correlation-energy formula into a functional of the electron density. Phys Rev B 37:785–789. https://doi.org/10.1103/PhysRevB.37.785

36. Chiodo S, Russo N, Sicilia E (2006) LANL2DZ basis sets recontracted in the framework of density functional theory. J Chem Phys 125:104107. https://doi.org/10.1063/1.2345197

37. Miessler GL, Fischer PJ, Tarr DA (2014) Inorganic Chemistry, 5th Edn. Pearson Education International, USA, 486-490.

38. Churchill MR, Amoh KN, Wasserman HJ (1981) Redetermination of the Crystal Structure of Dimanganese Decacarbonyl and Determination of the Crystal Structure of Dirhenium Decacarbonyl. Revised Values for the Mn-Mn and Re-Re Bond Lengths in $Mn_2(CO)_{10}$ and $Re_2(CO)_{10}$. Inorg Chem 20:1609–1611. https://doi.org/10.1021/ic50219a056

39. Chen J, Young VG, Angelici RJ (1996) Reactions of Cp*Ir(2,5-dimethylthiophene) with $Ru_3(CO)_{12}$, $Re_2(CO)_{10}$, $Mn_2(CO)_{10}$, and $[(\eta^6\text{-}C_6H_6)RuCl_2]_2$. Organometallics 15:2727–2734. https://doi.org/10.1021/om960078h

40. Casey CP, Cariño RS, Hayashi RK, Schladetzky KD (1996) Reaction of $Cp^*(CO)_2Re{=}Re(CO)_2Cp^*$ with dimethyl acetylenedicarboxylate produces a 3,4-dimetallacyclobutene which undergoes photochemical isomerization to a 2,4-dimetallabicyclo[1.1.0]butane. J Am Chem Soc 118:1617–1623. https://doi.org/10.1021/ja9515516

41. Adams RD, Perrin JL, Queisser JA, Wolfe JB (1997) Catalytic Macrocyclization of 3,3-Dimethylthietane by $Re_2(CO)_9(SCH_2CMe_2CH_2)$. Organometallics 16:2612–2617. https://doi.org/10.1021/om970162c

42. Adams RD, McBride KT, Rogers RD (1997) A new route to polyselenoether macrocycles. Catalytic macrocyclization of 3,3-dimethylselenetane by $Re_2(CO)_9SeCH_2CMe_2CH_2$. Organometallics 16:3895–3901. https://doi.org/10.1021/om970406t

43. Carlucci L, Proserpio DM, D'Alfonso G (1999) 1,2-eq,eq-$[Re_2(CO)_8(THF)_2]$: A reactive $Re_2(CO)_8$ fragment that easily activates H-H and C-H bonds. Organometallics

18:2091–2098. https://doi.org/10.1021/om9806693

44. Adams RD, Captain B, Hollandsworth CB, et al (2006) Synthesis and structures of oxo-bridged distannyl- And digermyldirhenium complexes. Organometallics 25:3848–3855. https://doi.org/10.1021/om060375e

45. Abdel-Magied AF, Patil MS, Singh AK, et al (2015) Synthesis, Characterization and Catalytic Activity Studies of Rhenium Carbonyl Complexes Containing Chiral Diphosphines of the Josiphos and Walphos Families. J Clust Sci 26:1231–1252. https://doi.org/10.1007/s10876-014-0809-y

46. Adams RD, Dhull P (2017) Formyl C-H activation in N,N-Dimethylformamide by a dirhenium carbonyl complex. J Organomet Chem 849–850:228–232. https://doi.org/10.1016/j.jorganchem.2017.03.009

47. Machado RA, Rivillo D, Arce AJ, et al (2004) Synthesis and molecular structure of $[Re_2(\mu{:}\eta^6\text{-}C_{24}H_{18}N_4)(CO)_6]$ containing the rtct-tetrakis(2-pyridyl) cyclobutandiyl ligand, derived from the reaction of $[Re_2(CO)_8(MeCN)_2]$ and 1,2-bis(2-pyridyl)ethene. J Organomet Chem 689:2486–2493. https://doi.org/10.1016/j.jorganchem.2004.05.005

48. Machado RA, Goite MC, Rivillo D, et al (2007) Reactivity of 2,3-bis(2-pyridyl)pyrazine with $[Re_2(CO)_8(CH_3CN)_2]$: Molecular structures of $[Re_2(CO)_8(C_{14}H_{10}N_4)]$ and $[Re_2(CO)_8(C_{14}H_{10}N_4)Re_2(CO)_8]$. J Organomet Chem 692:894–902. https://doi.org/10.1016/j.jorganchem.2006.10.042

49. Kabir SE, Ahmed F, Das A, et al (2008) Dirhenium carbonyl complexes bearing 2-vinylpyridine, morpholine and 1-methylimidazole ligands. J Organomet Chem 693:1696–1702. https://doi.org/10.1016/j.jorganchem.2007.09.023

50. Ghosh S, Ahmed F, Golzar Hossain GM, et al (2009) Reactivity of $[Re_2(CO)_8(MeCN)_2]$ with 1-vinylimidazole: X-ray Structures of $[Re_2(CO)_8Y\{\eta^1\text{-}NC_3H_3N(CH{=}CH_2)\}_2]$ and $[ReCl_2(CO)_2\{\eta^1\text{-}NC_3H_3N(CH{=}CH_2)\}_2]$. J Chem Crystallogr 39:702–707. https://doi.org/10.1007/s10870-009-9536-x

51. Peña D, Otero Y, Arce A, et al (2016) Synthesis, characterization and reactivity of dinuclear rhenium complexes containing hemilabile phosphines as ligands: X-ray structures of diax-$[Re_2(CO)_8\{\kappa^1(P)\text{-}Ph_2P(CH_2)_2CN\}_2]$, $[Re_2(CO)_8\{\mu{:}\kappa^3(P,C,C)\text{-}{}^iPr_2NP(CH_2CH{=}CH_2)_2\}]$ and diax-$[Re_2(CO)_8(PPh_3)\{\kappa^1(P)\text{-}p\text{-}MeOC_6H_4P(CH_2CH{=}CH_2)_2\}]$. Inorganica Chim Acta 439:178–185.

https://doi.org/10.1016/j.ica.2015.10.013

52. Otero Y, Arce A, Lescop C, et al (2019) High variety of coordination modes of π-conjugated phospholes in dinuclear rhenium carbonyls. Fluxional behavior of σ,π-complexes. Inorganica Chim Acta 491:118–127. https://doi.org/10.1016/j.ica.2019.04.008

53. Beltrán TF, Zaragoza G, Delaude L (2016) Synthesis, characterization, and gas-phase fragmentation of rhenium-carbonyl complexes bearing imidazol(in)ium-2-dithiocarboxylate ligands. Dalt Trans 45:18346–18355. https://doi.org/10.1039/c6dt03428d

54. Garcia R, Domingos Â, Paulo A, et al (2002) Reactivity of [Re{κ^3 -H(μ-H)B(tim Me)$_2$}(CO)$_3$] (tim Me = 2-Mercapto-1-methylimidazolyl) toward Neutral Substrates. Inorg Chem 41:2422–2428. https://doi.org/10.1021/ic011171n

55. Kabir SE, Ahmed F, Das A, et al (2007) Reactivity of [$Re_2(CO)_8(MeCN)_2$] with thiazoles: Hydrido bridged dirhenium compounds bearing thiazoles in different coordination modes. J Organomet Chem 692:4337–4345. https://doi.org/10.1016/j.jorganchem.2007.06.050

56. Tzeng BC, Chao A, Banik M (2014) Ligand-coupling assembly of Re(i)-thiolate complexes. Dalt Trans 43:11510–11515. https://doi.org/10.1039/c4dt00791c

57. Tzeng BC, Chao A, Lin MC, et al (2017) Molecular ReI Cages: Structural and Luminescent Properties. Chem - A Eur J 23:18033–18040. https://doi.org/10.1002/chem.201704122

58. Hao Z, Li N, Yan X, et al (2018) Synthesis, characterization and catalytic activities of rhenium carbonyl complexes bearing pyridine-alkoxide ligands. J Organomet Chem 870:51–57. https://doi.org/10.1016/j.jorganchem.2018.06.013

59. Świtlicka A, Choroba K, Szlapa-Kula A, et al (2019) Experimental and theoretical insights into spectroscopy and electrochemistry of Re(I) carbonyl with oxazoline-based ligand. Polyhedron 171:551–558. https://doi.org/10.1016/j.poly.2019.06.047

60. Das T, Rajak KK (2020) Synthesis, characterization and DFT studies of complexes bearing $[Re(CO)_3]^+$ core and reactivity towards cyanide ion. J Organomet Chem 908:121098. https://doi.org/10.1016/j.jorganchem.2019.121098

61. Tylicki RM, Wu W, Fanwick PE, Walton RA (1995) An Unsymmetrical Ligand

Arrangement in the Complex $Re_2(\mu\text{-}mp)_4Cl_2$ (mp = Monoanion of 2-Mercaptopyridine). Inorg Chem 34:988–991. https://doi.org/10.1021/ic00108a035

62. Bedier RA, Yousef TA, Abu El-Reash GM, El-Gammal OA (2017) Synthesis, structural, optical band gap and biological studies on iron (III), nickel (II), zinc (II) and mercury (II) complexes of benzyl α-monoxime pyridyl thiosemicarbazone. J Mol Struct 1139:436–446. https://doi.org/10.1016/j.molstruc.2017.03.054

63. Oueslati Y, Kansız S, Valkonen A, et al (2019) Synthesis, crystal structure, DFT calculations, Hirshfeld surface, vibrational and optical properties of a novel hybrid non-centrosymmetric material $(C_{10}H_{15}N_2)_2H_2P_2O_7$. J Mol Struct 1196:499–507. https://doi.org/10.1016/j.molstruc.2019.06.110

Figures

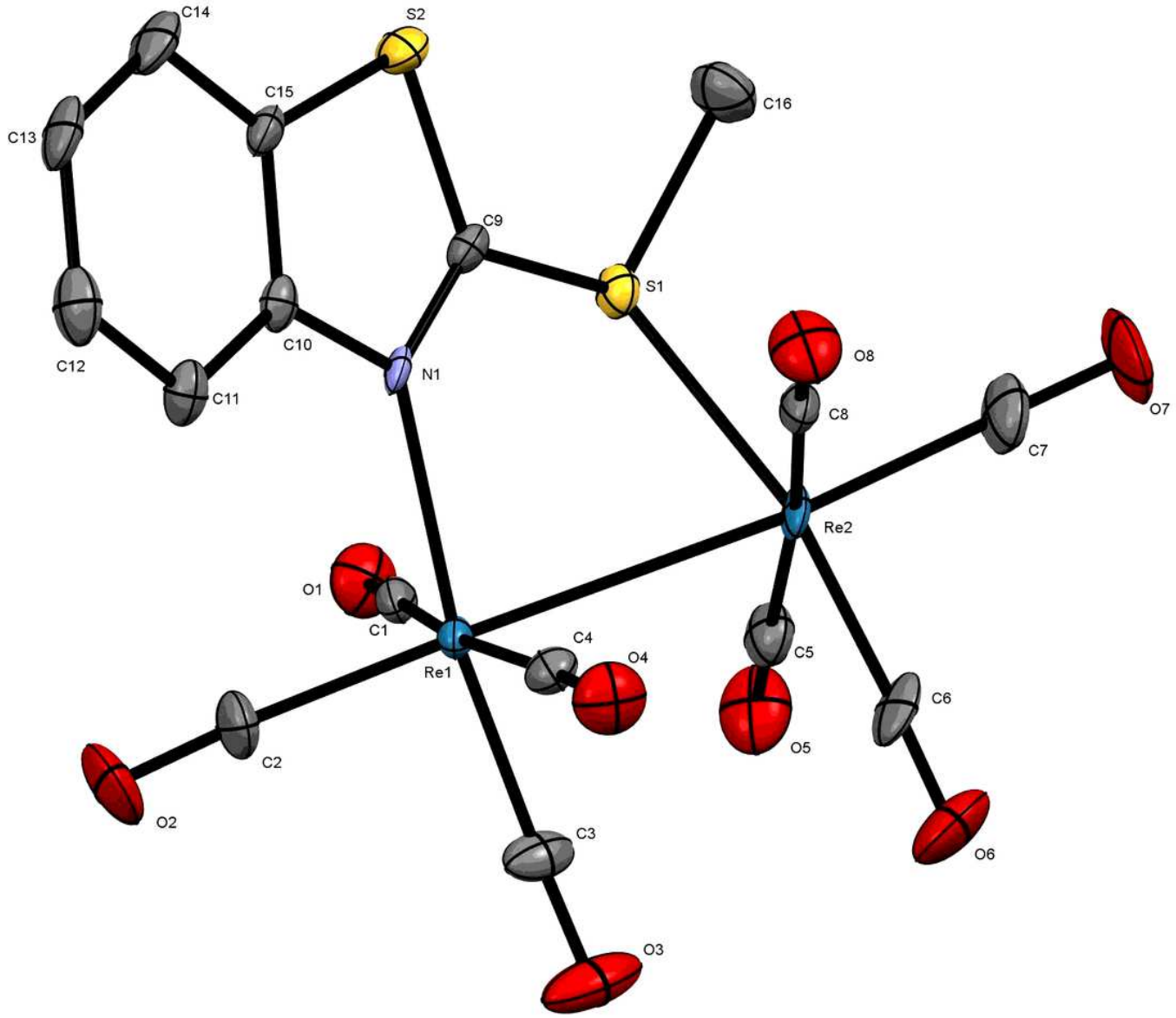

Figure 1

Solid-state molecular structure of [Re2(CO)8{μ,η1,η1-(CH3)SCNSC6H4}] (1). The atomic displacement ellipsoids are drawn at the 50% probability, and hydrogen atoms are omitted for clarity.

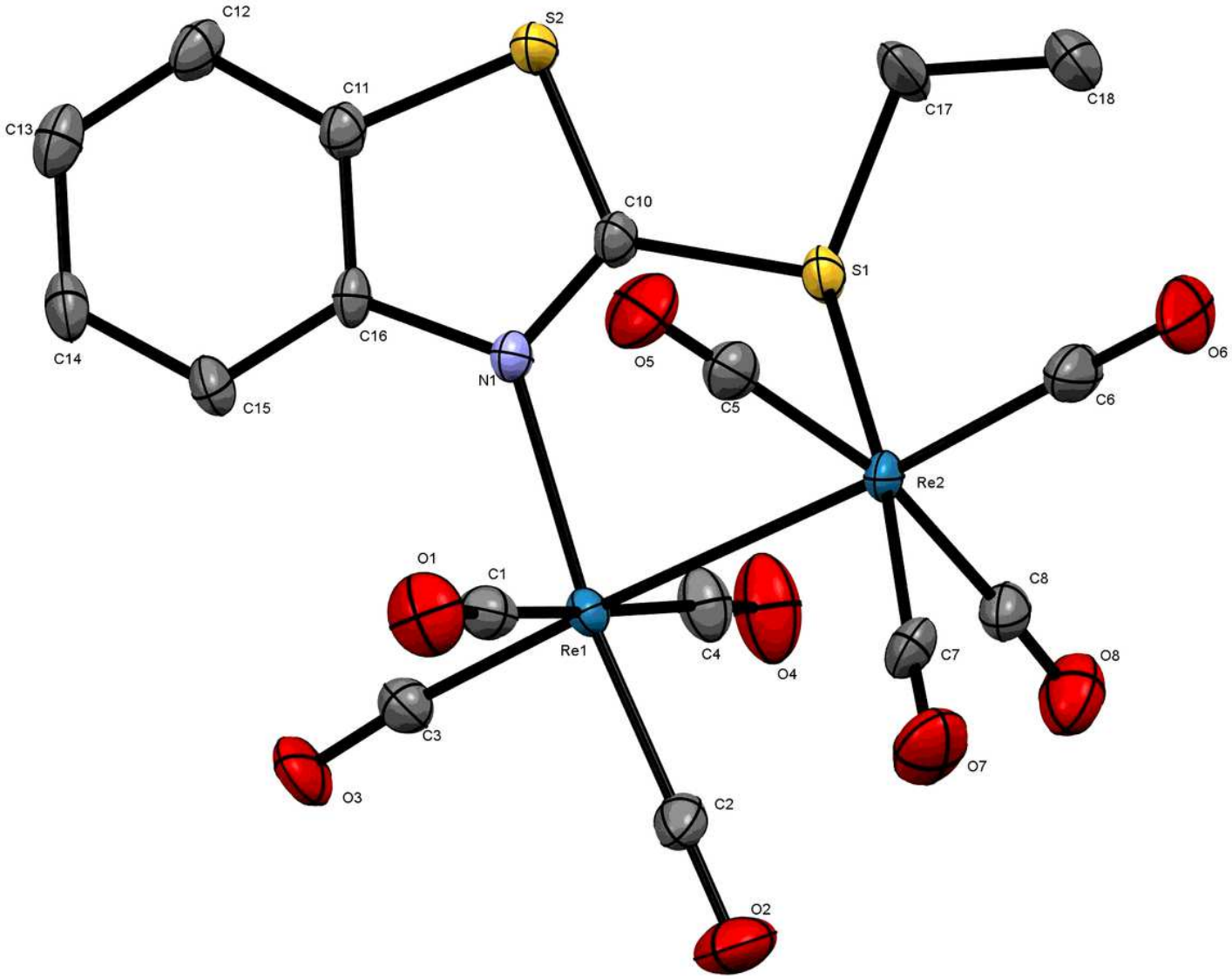

Figure 2

Solid state molecular structure of [Re2(CO)8{μ,η1,η1-(C2H5)SCNSC6H4}] (2). The atomic displacement ellipsoids are drawn at the 50% probability, and hydrogen atoms are omitted for clarity.

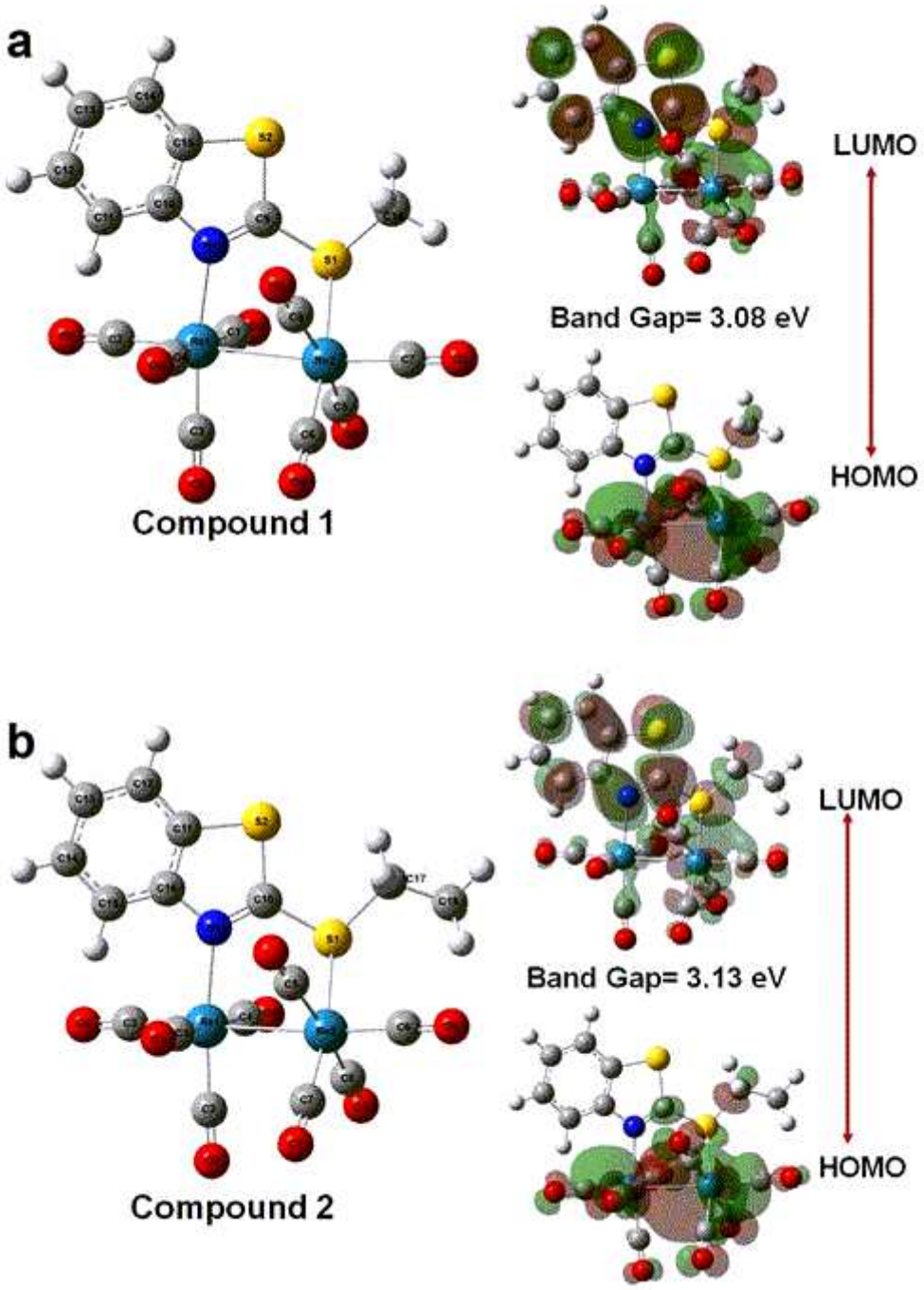

Figure 3

Optimized structures and calculated frontier molecular orbitals of (a) compound 1 and (b) compound 2

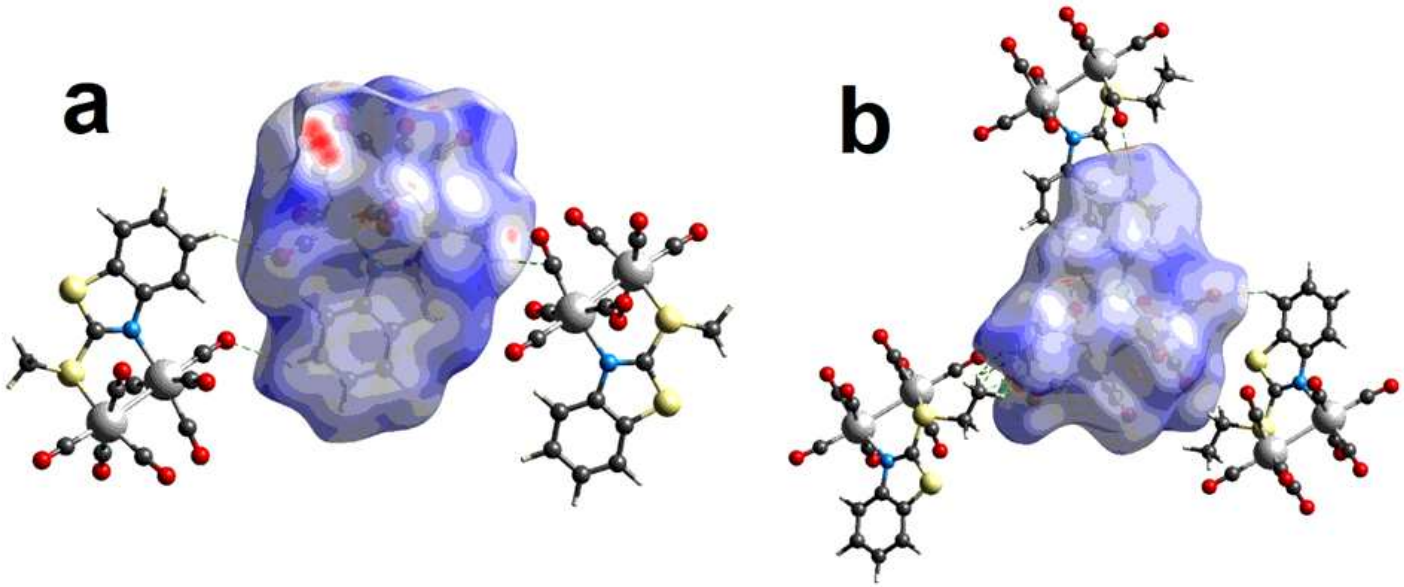

Figure 4

Perspective view of the dnorm Hirshfeld surfaces of (a) compound 1 and (b) compound 2

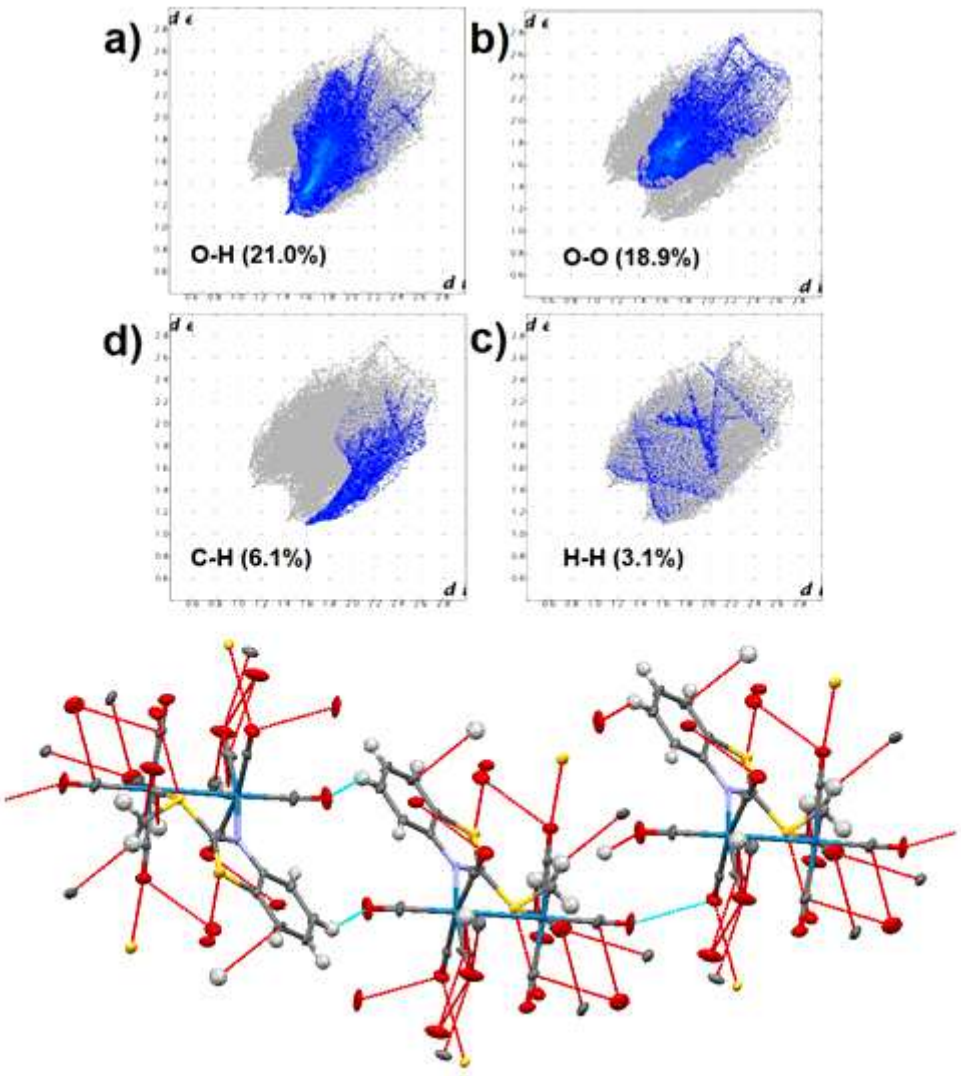

Figure 5

2D fingerprint plots showing the main close contact contributions (%) for a) O—H, b) O—O, c) H—H and d) C—H on the Hirshfeld surface area (top), and observed close contact (bottom) for compound 1.

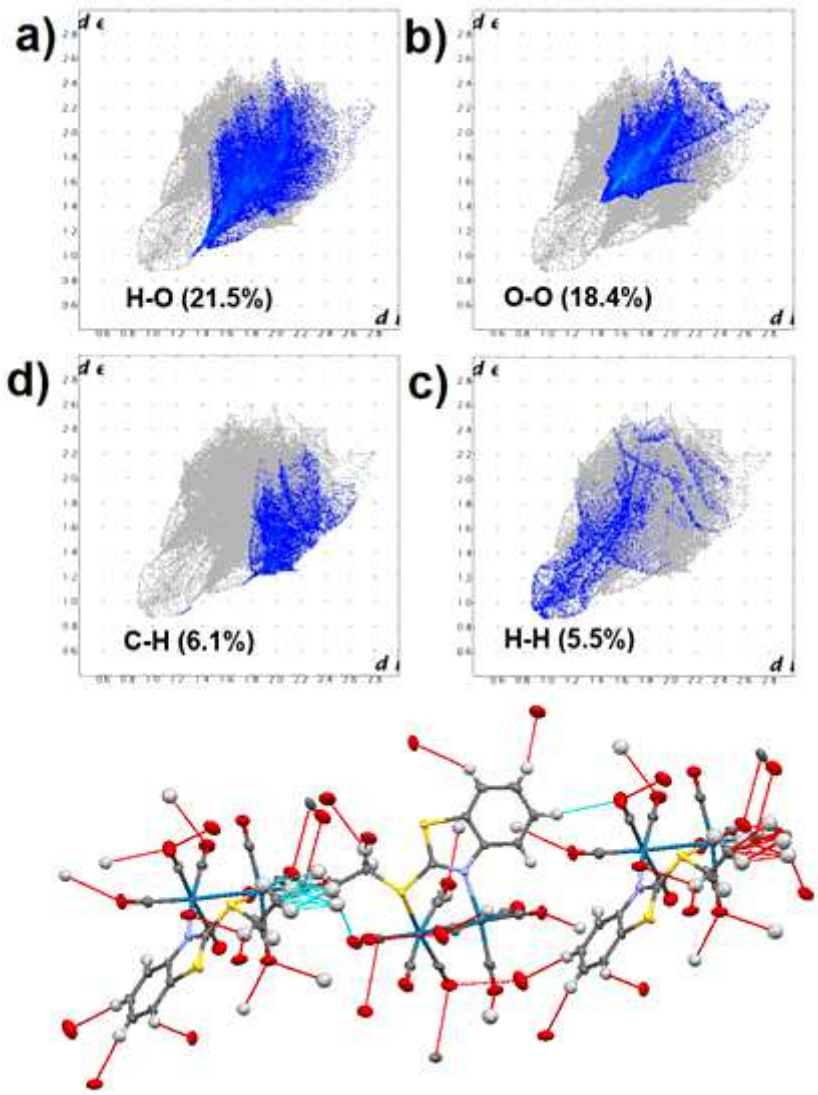

Figure 6

2D fingerprint plots showing the main close contact contributions (%) for a) O—H, b) O—O, c) H—H and d) C—H on the Hirshfeld surface area (top), and observed close contact (bottom) for compound 2.

Supplementary Files

This is a list of supplementary files associated with this preprint. Click to download.

- GraphicalAbstract.tif
- Chart01.png
- Chart02.png
- Chart03.png
- Scheme01.png